



HAL
open science

Analysis of the faster-than-Nyquist optimal linear multicarrier system

Alexandre Marquet, Cyrille Siclet, Damien Roque

► **To cite this version:**

Alexandre Marquet, Cyrille Siclet, Damien Roque. Analysis of the faster-than-Nyquist optimal linear multicarrier system. *Comptes Rendus. Physique*, 2017, Energy and radiosciences, 18 (2), pp.168-177. 10.1016/j.crhy.2016.11.006 . hal-01442085

HAL Id: hal-01442085

<https://hal.science/hal-01442085>

Submitted on 20 Jan 2017

HAL is a multi-disciplinary open access archive for the deposit and dissemination of scientific research documents, whether they are published or not. The documents may come from teaching and research institutions in France or abroad, or from public or private research centers.

L'archive ouverte pluridisciplinaire **HAL**, est destinée au dépôt et à la diffusion de documents scientifiques de niveau recherche, publiés ou non, émanant des établissements d'enseignement et de recherche français ou étrangers, des laboratoires publics ou privés.



ELSEVIER

Contents lists available at ScienceDirect

Comptes Rendus Physique

www.sciencedirect.com



Energy and radiosciences / Énergie et radiosciences

Analysis of the faster-than-Nyquist optimal linear multicarrier system

*Analyse du système linéaire optimal pour les communications multiporteuses au-delà de la cadence de Nyquist*Alexandre Marquet^{a,*}, Cyrille Siclet^a, Damien Roque^b^a Université Grenoble Alpes, CNRS, GIPSA-Lab, 38000 Grenoble, France^b Institut supérieur de l'aéronautique et de l'espace (ISAE-SUPAERO), Université de Toulouse, 31055 Toulouse, France

ARTICLE INFO

Article history:

Available online 19 December 2016

Keywords:

Multicarrier modulations
Faster-than-Nyquist signaling
Interference analysis
Performance analysis

Mots-clés :

Modulations multiporteuses
Transmission au-delà de la cadence de Nyquist
Analyse de l'interférence
Analyse des performances

ABSTRACT

Faster-than-Nyquist signalization enables a better spectral efficiency at the expense of an increased computational complexity. Regarding multicarrier communications, previous work mainly relied on the study of non-linear systems exploiting coding and/or equalization techniques, with no particular optimization of the linear part of the system. In this article, we analyze the performance of the optimal linear multicarrier system when used together with non-linear receiving structures (iterative decoding and direct feedback equalization), or in a standalone fashion. We also investigate the limits of the normality assumption of the interference, used for implementing such non-linear systems. The use of this optimal linear system leads to a closed-form expression of the bit-error probability that can be used to predict the performance and help the design of coded systems. Our work also highlights the great performance/complexity trade-off offered by decision feedback equalization in a faster-than-Nyquist context.

© 2016 Académie des sciences. Published by Elsevier Masson SAS. This is an open access article under the CC BY-NC-ND license

(<http://creativecommons.org/licenses/by-nc-nd/4.0/>).

R É S U M É

Les communications au-delà de la cadence de Nyquist permettent une augmentation de l'efficacité spectrale en contrepartie d'une complexité plus élevée. Concernant les communications multiporteuses, les travaux menés jusque-là se sont principalement focalisés sur l'étude des systèmes non linéaires exploitant des techniques de codage et/ou d'égalisation, sans considération ou optimisation particulière de la partie linéaire du système. Dans cet article, nous analysons le comportement du système linéaire multiporteuse optimal lorsqu'il est utilisé seul ou avec des structures de réception non linéaires (décodage itératif et égalisation à retour de décision). Nous nous intéressons également aux limites de l'hypothèse de normalité de l'interférence, laquelle est utilisée lors de l'implémentation de ces systèmes non linéaires. L'utilisation du système linéaire optimal permet d'obtenir une expression analytique de la probabilité d'erreur, laquelle peut alors être utilisée pour prédire les performances et aider à la conception de systèmes codés. Ce travail met aussi en avant le bon compromis performances/complexité offert par

* Corresponding author.

E-mail addresses: alexandre.marquet@gipsa-lab.fr (A. Marquet), cyrille.siclet@gipsa-lab.fr (C. Siclet), damien.roque@isae-supaero.fr (D. Roque).

l'égaliseur à retour de décision dans le contexte des communications au-delà de la cadence de Nyquist.

© 2016 Académie des sciences. Published by Elsevier Masson SAS. This is an open access article under the CC BY-NC-ND license (<http://creativecommons.org/licenses/by-nc-nd/4.0/>).

1. Introduction

Most current communication systems enable perfect reconstruction of the transmitted symbols: synthesis and analysis families, used respectively for transmission and reception, are biorthogonal (they are Riesz bases). In the scope of bandlimited transmission, this is only guaranteed when the Nyquist criterion is respected, which imposes a symbol rate R lower than the bilateral bandwidth B ($R \leq B$) [1]. On the contrary, overriding this criterion makes it possible to transmit at a higher symbol rate R' while keeping the same bandwidth ($R' > B$), which improves *spectral efficiency* (defined as the ratio between the bitrate of the transmission D and the bilateral bandwidth B of the signal). However, this technique, referred to as *faster-than-Nyquist* (FTN), induces an interference between pulse-shapes (or inter-pulse-interference – IPI).

In a context of overcrowded radiofrequency resources, FTN communications allow for a reduction of the spectral occupancy at a given bitrate or, equivalently, for a higher bitrate at a given spectral occupancy. Unlike a more classical way to improve spectral efficiency consisting in an augmentation of the modulation alphabet's size (every other parameters being fixed), FTN systems do not rise the sensitivity to the noise if IPI is properly compensated at the receiver's side. Moreover, lots of transmission systems are designed to work with multipath, and potentially mobile, channels. Through such channels, multicarrier modulations are particularly efficient as they permit to choose matched pulse-shapes according to the time–frequency selectivity of the channel, thus reducing equalization complexity at the receiver's size [2]. FTN transmission technique can be extended to this family of modulations [3]. In this case, denoting T_0 the multicarrier symbol duration and F_0 the inter-carrier spacing, one can show that transmission and reception families are no longer biorthogonal if $F_0 T_0 < 1$ (they can, however, form overcomplete frames), which leads to IPI in both time and frequency.

This article is based on the use of the optimal multicarrier linear system with respect to the signal-to-interference-plus-noise ratio (SINR) criterion, as developed in [4], and which relies on the use of tight Gabor frames in transmission and reception. We will investigate the performance of this system in combination with decision feedback equalization (DFE) and low-density parity check coding (LDPC).

This article is constructed as follows. Section 2 presents the input–output relations of the system, based on frame theory. This theoretical framework allows for the determination of the SINR, as well as the closed-form expression of the bit-error probability for a transmission over an additive white Gaussian noise (AWGN) channel. Section 3 goes into the details of two interference mitigation techniques. The first one is based on a LDPC code, while the other one uses a DFE structure. Section 4 underlines the limits of the Gaussian approximation of the interference by means of simulations and then presents the performance of the two interference mitigation structures mentioned in Section 3. Conclusion and perspectives are finally given in Section 5.

2. Optimal linear multicarrier system with AWGN

2.1. Input–output relation of the linear multicarrier system

We denote $\mathbf{c} = \{c_{m,n}\}_{(m,n) \in \Lambda} \in \ell_2(\Lambda)$ a sequence of zero-mean, independent, and identically distributed (IID) coefficients, with variance σ_c^2 and $\Lambda \subset \mathbf{Z}^2$. The equivalent baseband multicarrier signal is defined by

$$s(t) = \sum_{(m,n) \in \Lambda} c_{m,n} g_{m,n}(t), \quad t \in \mathbf{R} \quad (1)$$

with $\mathbf{g} = \{g_{m,n}\}_{(m,n) \in \Lambda}$ a Gabor family with parameters $F_0, T_0 > 0$ and whose elements are given by its generator $g(t) \in \mathcal{L}_2(\mathbf{R})$:

$$g_{m,n}(t) = g(t - nT_0) e^{j2\pi m F_0 t} \quad (2)$$

As a consequence, the information carried by \mathbf{c} is regularly spread in the time–frequency plane (Fig. 1) with a minimal distance F_0 in frequency and T_0 in time.

In practice, the transmission is limited to M subcarriers and K symbols such that $\Lambda = \{0, \dots, M-1\} \times \{0, \dots, K-1\}$ is a finite set, inducing that the sum (1) always converges. It can however possess a lot of terms, so it is important to ensure its stability. Denoting $\mathcal{H}_{\mathbf{g}} = \overline{\text{Vect}(\mathbf{g})}$ the closure of the linear span of the family \mathbf{g} ,¹ the stability of (1) is guaranteed when \mathbf{g} is a Bessel sequence, which means that there exists a bound $B_{\mathbf{g}} > 0$ such that

¹ The closure of a normed vector space \mathbf{E} contains all the elements of \mathbf{E} , together with its limit elements. For example, the closure of the set of the rational numbers is the set of the real numbers.

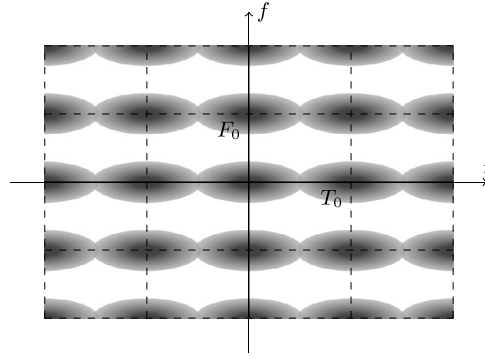


Fig. 1. Time–frequency representation of a multicarrier signal. In this example, the generator $g(t)$ and the parameters T_0 and F_0 are chosen in order to show a clear separation in frequency, but not in time.

$$\sum_{(m,n) \in \Lambda} | \langle g_{m,n}, x \rangle |^2 \leq B_g \|x\|^2 \quad \forall x \in \mathcal{H}_g \quad (3)$$

with $\langle \cdot, \cdot \rangle$ and $\|\cdot\|$ the usual inner product and norm of $\mathcal{L}_2(\mathbf{R})$, defined by

$$\langle x, y \rangle = \int_{-\infty}^{+\infty} x^*(t)y(t) dt, \quad \|x\| = \sqrt{\langle x, x \rangle} \quad \forall x, y \in \mathcal{L}_2(\mathbf{R}) \quad (4)$$

where \cdot^* denotes the complex conjugation. To perfectly reconstruct \mathbf{c} from the knowledge of $s(t)$, it is furthermore necessary (and sufficient) for \mathbf{g} to be a linearly independent family. \mathbf{g} is then a Riesz basis of \mathcal{H}_g , in other words a linearly independent family for which there exist two bounds $0 < A_g \leq B_g$ such that:

$$A_g \|x\|^2 \leq \sum_{(m,n) \in \Lambda} | \langle g_{m,n}, x \rangle |^2 \leq B_g \|x\|^2 \quad \forall x \in \mathcal{H}_g \quad (5)$$

The density ρ of \mathbf{g} must then be lower than or equal to one: $\rho = 1/(F_0 T_0) \leq 1$. In this article, we take the opposite case where $\rho > 1$ in order to rise the spectral efficiency of the system (every other parameters being fixed). For a linear receiver, this interference is considered as an additive noise, added to the one induced by the channel, yielding to a higher error probability. However, when $\rho > 1$, there exist linearly dependent Gabor families, which constitute redundant frames of $\mathcal{L}_2(\mathbf{R})$. These are families for which (5) is valid for $x \in \mathcal{L}_2(\mathbf{R})$. As a consequence, the stability of (1) is always guaranteed and $\mathcal{H}_g = \mathcal{L}_2(\mathbf{R})$, but \mathbf{g} cannot be a basis of $\mathcal{L}_2(\mathbf{R})$.

We suppose a perfect channel with additive noise and we specify a linear receiver such that \mathbf{c} is estimated by

$$\hat{c}_{p,q} = \langle \check{g}_{p,q}, r \rangle \quad \forall (p, q) \in \Lambda \quad (6)$$

with $\check{\mathbf{g}} = \{\check{g}_{m,n}\}_{(m,n) \in \Lambda}$ a reception family, $r(t) = s(t) + z(t)$ the received signal and $z(t)$ a zero-mean white Gaussian complex circular noise, independent of the symbols and characterized by its power spectral density $\gamma_z(f) = 2N_0$ for $f \in \mathbf{R}$: $E(z(t)) = 0$ and $E(z^*(t)z(t')) = 2N_0\delta(t - t')$, with $E(\cdot)$ the expectation operator.

2.2. Interference and noise analysis

It is possible to rewrite (6) in order to highlight interference and noise terms:

$$\hat{c}_{p,q} = \underbrace{c_{p,q} \langle \check{g}_{p,q}, g_{p,q} \rangle}_{\check{c}_{p,q}: \text{useful signal}} + \underbrace{\sum_{(m,n) \in \Lambda \setminus \{(p,q)\}} c_{m,n} \langle \check{g}_{p,q}, g_{m,n} \rangle}_{i_{p,q}: \text{interference}} + \underbrace{\langle \check{g}_{p,q}, z \rangle}_{z_{p,q}: \text{noise}} \quad (7)$$

In [4] we showed that the SINR is maximized when $\check{\mathbf{g}} = 1/A_g \mathbf{g}$ is a tight frame, which means that (5) is true with $A_g = B_g$. In that case, the following relations hold:

$$\|\mathbf{g}\|^2 = A_g / \rho \quad (8)$$

$$E_s = \frac{A_g}{2\rho} \sigma_c^2 \quad (9)$$

$$\sigma_i^2 = E(|i_{p,q}|^2) = (\rho - 1) \sigma_c^2 \quad (10)$$

$$\sigma_z^2 = E(|z_{p,q}|^2) = \frac{\rho}{A_g} 2N_0 \quad (11)$$

with E_s the per-symbol energy, σ_i^2 the interference's variance and σ_z^2 the noise's variance after filtering, so that the SINR can be written as follows:

$$\text{SINR} = \frac{1}{\rho - 1 + \frac{N_0}{E_s}} \quad (12)$$

We observe that the interference term $i_{p,q}$ is a random variable independent of the noise, and that it corresponds to the sum of a high number of zero-mean, independent random variables $\tilde{c}_{m,n}$ following the same kind of distribution, but having different variances $\sigma_{\tilde{c}_{m,n}}^2$:

$$\tilde{c}_{m,n} = c_{m,n} \langle \check{g}_{p,q}, \mathbf{g}_{m,n} \rangle \quad \text{and} \quad \sigma_{\tilde{c}_{m,n}}^2 = \sigma_c^2 |\langle \check{g}, \mathbf{g}_{m-p,n-q} \rangle|^2 \quad (13)$$

The necessary conditions to apply the central limit theorem are thus not fulfilled. This is confirmed by our simulations in Section 4.1, which show that the interference does not exactly follow a normal distribution. However, we notice that it is a good approximation when $\rho \leq 8/5$. In this scenario, the transmission becomes similar to a case were the symbols would have been transmitted over a non-dispersive channel with AWGN, and a signal-to-noise ratio equal to (12). Regarding the filtered noise term $z_{p,q}$, it is worthwhile noting that it is zero-mean Gaussian, but not necessarily white.

2.3. Approximation of the bit-error probability

We now restrict ourselves to the case where the symbols \mathbf{c} are chosen from a quadrature phase-shift keying (QPSK) alphabet. In this case, considering both the interference and the noise to be Gaussian, the theoretical error probability for a transmission over a perfect channel with AWGN is given by the following formula:

$$P_e = Q\left(\sqrt{\text{SINR}}\right) = Q\left(\sqrt{\frac{1}{(\rho - 1) + \frac{N_0}{2E_b}}}\right) \quad (14)$$

with $Q(\cdot)$ the complementary cumulative distribution function (CCDF) of the standard normal distribution and $E_b = E_s/2$ the per-bit energy [5, chapter 4].

3. Interference mitigation structures

3.1. LDPC forward error correction

By considering the interference as a noise, a straightforward reception strategy relies on the compensation of both the noise and the interference by channel coding. In this work, we choose a LDPC code because of its good correcting capabilities at a given coding rate (see Section 4.3 for simulation results). Decoders for this family of codes rely on algorithms using soft inputs in the form of log-likelihood ratios (LLR), given by

$$L(b_l(c_{p,q})|\hat{c}_{p,q}) = \ln \left(\frac{\Pr\{b_l(c_{p,q}) = 0|\hat{c}_{p,q}\}}{\Pr\{b_l(c_{p,q}) = 1|\hat{c}_{p,q}\}} \right) \quad (15)$$

where $b_l(c_{p,q})$ is the l th bit of symbol $c_{p,q}$. Using the Gaussian approximation of the interference, it is possible to write the probability density function (PDF) of the sum of the noise and the interference term $v_{p,q} = z_{p,q} + i_{p,q}$ as:

$$f_v(x) = \frac{1}{\pi\sigma_v^2} \exp\left(\frac{-|x|^2}{\sigma_v^2}\right) \quad (16)$$

where, given (10) and (11)

$$\sigma_v^2 = \sigma_z^2 + \sigma_i^2 = (\rho - 1)\sigma_c^2 + \frac{\rho}{A_g} 2N_0 \quad (17)$$

Moreover, from (7) and (8), one can write $v_{p,q} = \hat{c}_{p,q} - c_{p,q}/\rho$, which, given that the symbols are IID, following a uniform distribution, leads to

$$L(b_l(c_{p,q})|\hat{c}_{p,q}) = \ln \left(\frac{\sum_{c \text{ s.t. } b_l(c)=0} \exp\left(\frac{-|\hat{c}_{p,q}-c/\rho|^2}{\sigma_v^2}\right)}{\sum_{c \text{ s.t. } b_l(c)=1} \exp\left(\frac{-|\hat{c}_{p,q}-c/\rho|^2}{\sigma_v^2}\right)} \right) \quad (18)$$

Simulations of Section 4.3 use LLR computed via (18), meaning that we suppose that the PDF of the interference is well approximated by a Gaussian function, which, as shown in Section 4.1, is relevant for $\rho \leq 8/5$.

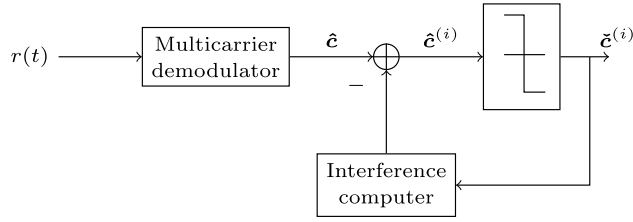


Fig. 2. Flowchart of a receiver exploiting our proposed per-block iterative DFE. $\hat{\mathbf{c}}$, $\hat{\mathbf{c}}^{(i)}$ and $\check{\mathbf{z}}^{(i)}$ are matrices containing the elements $\hat{c}_{p,q}$, $\hat{c}_{p,q}^{(i)}$, $\check{z}_{p,q}^{(i)}$ respectively (where p indexes the lines and q the columns).

3.2. Decision feedback equalization

Another way to mitigate interference relies on equalization schemes. In this part, we derive an equalization structure that uses previously estimated symbols to cancel the interference term. Indeed, as shown in (7), if this term is completely canceled, then the performance of the FTN system is identical to that of an orthogonal system (i.e. a system with density $\rho \leq 1$) in terms of bit error rate (BER).

Let us suppose that the generator $g(t)$ used in transmission is known by the receiver, then the only missing parameter to compute the interference term $i_{p,q}$ is the transmitted symbols sequence \mathbf{c} . The DFE presented here uses a per-block iterative approach: symbols obtained after thresholding at the previous iteration are used to compute and remove the interference term in the current iteration (Fig. 2). Estimated symbols after interference cancellation are given by

$$\hat{c}_{p,q}^{(i)} = c_{p,q} \langle \check{g}_{p,q}, g_{p,q} \rangle + \sum_{(m,n) \in \Lambda \setminus \{(p,q)\}} (c_{m,n} - \check{c}_{m,n}^{(i-1)}) \langle \check{g}_{p,q}, g_{m,n} \rangle + \langle \check{g}_{p,q}, z \rangle, \quad i \in \{0, \dots, N_I - 1\} \quad (19)$$

where N_I is the total number of iterations, $\hat{c}_{p,q}^{(i)}$ and $\check{c}_{p,q}^{(i)}$ are respectively the symbols estimated and the symbols obtained after thresholding at iteration i . In the first iteration, we set $\check{c}_{p,q}^{(-1)} = 0$ so that $\hat{c}_{p,q}^{(0)} = \hat{c}_{p,q}$, $(p, q) \in \Lambda$.

We can see that in the perfect case, where the symbols after the threshold detector at iteration $i - 1$ are identical to the symbols sent ($\check{c}_{p,q}^{(i-1)} = c_{p,q}$, $(p, q) \in \Lambda$), the interference term is completely removed at iteration i . However, this is never the case in practice since error propagation occurs (BER floor at high SNR).

4. Simulations on AWGN channel

4.1. Empirical analysis of the interference

As introduced in 2.2, it is necessary to empirically study the statistical properties of the interference. To this extent, we measured 3.6×10^6 realizations of the interference term $i_{p,q}$ through the transmission of $K = 50000$ multicarrier symbols taking their values in a QPSK alphabet, over $M = 128$ subcarriers, using transmission and reception generators yielding tight frames, for different values of the density ρ and over a perfect noise-free channel. These realizations of the interference term were then standardized in order to facilitate the comparison of their cumulative distribution function (CDF) and PDF to the standard Gaussian distribution's one. We observed a similar statistical behavior for both the real and imaginary parts of $i_{p,q}$, as well as various generator functions yielding tight frames.

Considering the transmission of IID bits over a perfect noise-free channel ($\text{SINR} = 1/(\rho - 1)$) and denoting $F_{i,\rho}(x)$ the CDF of the interference for a density ρ , one can express the bit-error probability as

$$P_e(\rho) = 1 - F_{i,\rho}(\sqrt{\text{SINR}}) = 1 - F_{i,\rho}\left(\sqrt{\frac{1}{\rho - 1}}\right) \quad (20)$$

In order to evaluate the validity of the Gaussian approximation of the interference in the context of error probability estimation, we compare $P_e(\rho)$ and $Q(\sqrt{1/(\rho - 1)})$ for various values of ρ in Fig. 3. We can see that, although it does not strictly follow a Gaussian distribution, such an approximation appropriately fits the bit-error probability given $\rho > 16/15$. Moreover, when $\rho \leq 16/15$ the Q-function seems to be an upper bound of the bit-error probability.

In order to verify the relevance of this approximation for computing LLR used by soft-input reception algorithms (such as LDPC decoders), we compare the PDF of the interference $f_{i,\rho}(x)$ to the one of a standard Gaussian distribution $f_{\mathcal{N}(0,1)}(x)$ for various values of the density in Fig. 4. We see that the Gaussian approximation is relevant for the interference PDF's estimation given $\rho \leq 8/5$. However, for higher values of the density, the approximation error can become sufficiently high to introduce significant errors when computing LLR, yielding degraded performance.

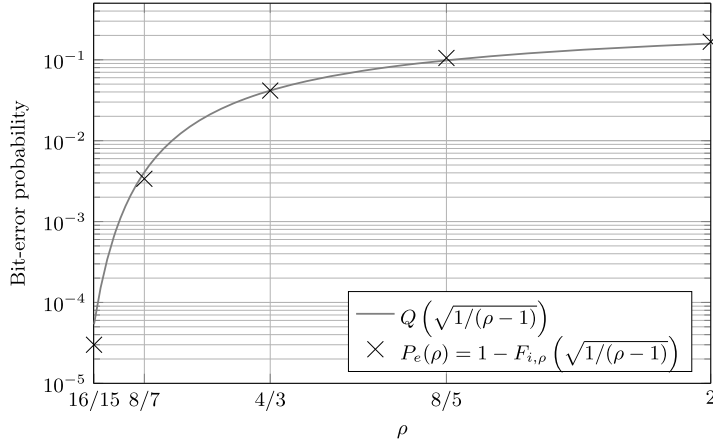


Fig. 3. Comparison of the CCDF of the interference and its Gaussian approximation (Q-function) with respect to the density ρ .

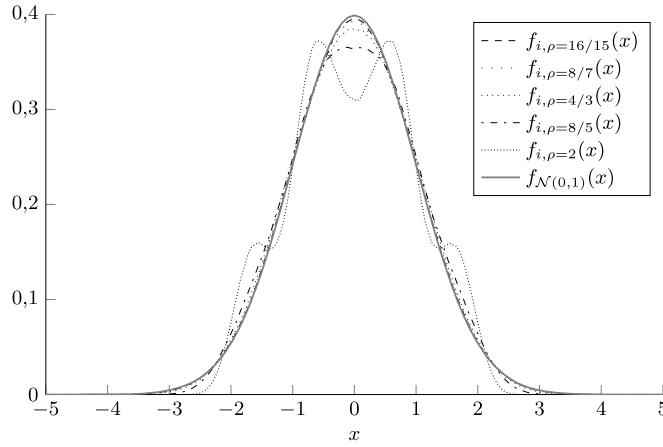


Fig. 4. Comparison of the PDF of the interference and its Gaussian approximation with respect to the density ρ .

4.2. Linear system performance

Simulations in this Section as well as in Sections 4.3 and 4.4 make use of transmissions of $K = 5000$ multicarrier symbols over $M = 128$ subcarriers with a QPSK constellation. They were run for various generators (yielding tight frames or not). Tight frames are obtained using the duality principle of the Wexler–Raz theorem [6, Theorem 9.3.4]. Indeed, this theorem states that g and \check{g} generate dual Gabor frames with time–frequency parameters T_0, F_0 if and only if they generate biorthogonal Riesz–Gabor sequences with time–frequency parameters $1/F_0, 1/T_0$. What is more, g generates a tight Gabor frame with time–frequency parameters T_0, F_0 if and only if it generates an orthogonal Gabor sequence with parameters $1/F_0, 1/T_0$. Thus, orthogonal generators used in the case $\rho < 1$ correspond to tight frame generators when $\rho > 1$. Thus, the two orthogonal generators obtained in [7] form tight frames, as shown in [4]. The first one, which maximizes the time–frequency localization is denoted by TFL, and the second one, which minimizes the out-of-band energy is denoted as OBE. For the same reasons, the square-root-raised-cosine (SRRC) with the roll-off factor $\alpha = \rho - 1$ as well as the T_0 -width rectangular (RECT_{T_0}) generator yield tight frames. When such a generator is used in both transmission and reception, it is sufficient to set its norm to $1/\sqrt{\rho}$ in order to obtain tight frames with $A_g = 1$. By contrast, although the $\text{RECT}_{\rho T_0}$ and RECT_{T_0} generates dual frames, they are not canonical dual and using one of them for transmission and the other for reception does not lead to a pair of tight frames. Finally, the rectangular generator of width ρT_0 ($\text{RECT}_{\rho T_0}$) does not form canonical dual frames when used both in transmission and reception.

Fig. 5 shows that the SINR is perfectly predicted by (12) when transmission and reception generators yield tight dual canonical frames. Performance gets worse when this condition is not respected, which is in line with the results shown in [4]. In this case, we can see that it is better to use the same families for transmission and reception, even if they are not dual frames, than using non-tight dual frames.

Fig. 6 confirms the relevance of the closed-form expression of the bit-error probability (14). It means that the Gaussian approximation of the interference term is also accurate, even for $\rho > 8/5$, because in this case, the BER is sufficiently high compared to the approximation error so that the relative error is kept low. However, for strong values of E_b/N_0

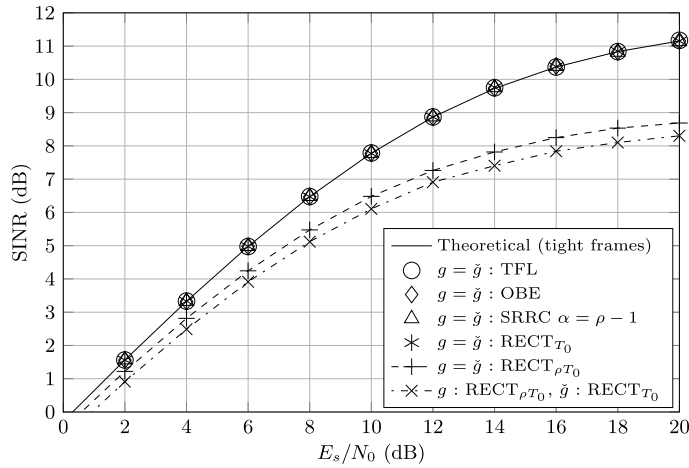


Fig. 5. SINR versus E_s/N_0 , with $\rho = 16/15$.

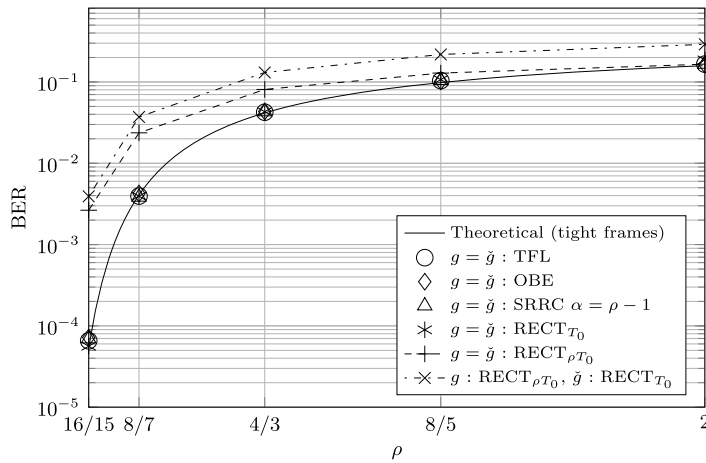


Fig. 6. BER versus ρ , with $E_b/N_0 = 20$ dB.

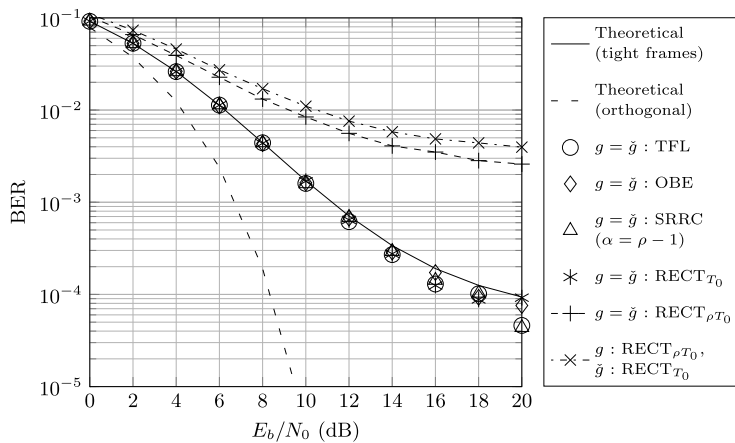


Fig. 7. BER versus E_b/N_0 , with $\rho = 16/15$.

(≥ 14 dB) and for ρ close to one ($\rho = 16/15$), the limits of this approximation become noticeable (Fig. 7). In the context of a non-coded system, the BER rapidly increases with the density (Fig. 6), and a lower bound of the BER appears when the noise power becomes negligible compared to the interference's one (Fig. 7). These results confirm the need for non-linear detectors enabling a better interference mitigation.

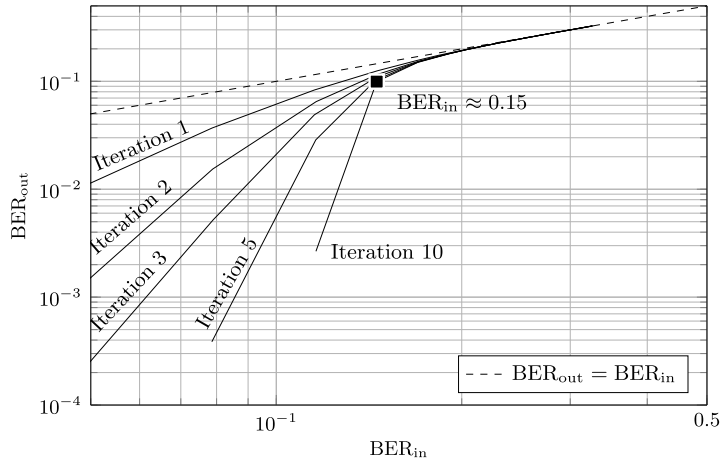


Fig. 8. Output BER as a function of the input BER for the rate 1/2 LDPC code of the DVB-S2 standard over an AWGN channel. In this configuration, the convergence threshold is given at $BER_{in} = 0.15$.

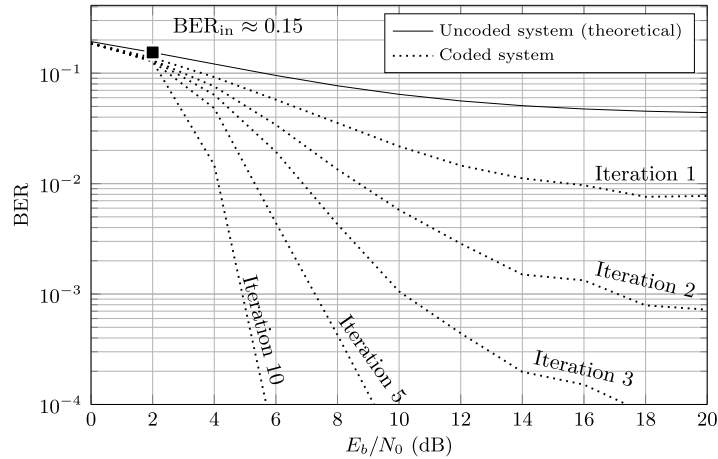


Fig. 9. BER as a function of E_b/N_0 for a system using the rate 1/2 LDPC code of the DVB-S2 standard (10 iterations of the decoder), a density $\rho = 4/3$ and a TFL generator. The convergence threshold happens at the value of E_b/N_0 corresponding to the expected BER_{in} (determined using Fig. 8).

4.3. Performance with LDPC coding

BER curves of coded systems using iterative structures such as turbo-codes or LDPC are characterized by their so-called *convergence threshold* corresponding to the lowest E_b/N_0 value allowing a better BER at the output of the decoder (denoted as BER_{out}) than at its input (denoted as BER_{in}) [8]. For transmissions happening over a perfect channel with AWGN, it is also possible to characterize such a coded system with a curve representing BER_{out} as a function of BER_{in} . On this kind of curve, the convergence threshold is given with a particular value of the input BER. As a consequence, thanks to the closed-form expression of the error probability given in (14), one can find the highest density ρ allowing the coded system to converge for a given value of E_b/N_0 .

For instance, Fig. 8 shows that a system using the rate 1/2 LDPC code defined in the DVB-S2 standard [9] has its convergence threshold for an input BER of approximately 0.15. Referring to the Fig. 9, we can see that when this code is used together with a multicarrier FTN system using tight frames, the convergence threshold happens for $E_b/N_0 = 2$ dB, which actually is the signal-to-noise ratio corresponding to an input BER of 0.15.

4.4. Performance with direct feedback equalization

Our proposed per-block iterative DFE, although its very low complexity, can effectively mitigate interference for low SNR values, yielding close proximity between FTN multicarrier DFE and orthogonal system BER performance, as shown by Fig. 10. We observe that the BER performance of this DFE does not depend on the generators used in transmission and reception as long as they yield tight canonical dual frames. For strong values of E_b/N_0 , we can see the error propagation phenomenon as the BER becomes constant while the noise power is decreasing.

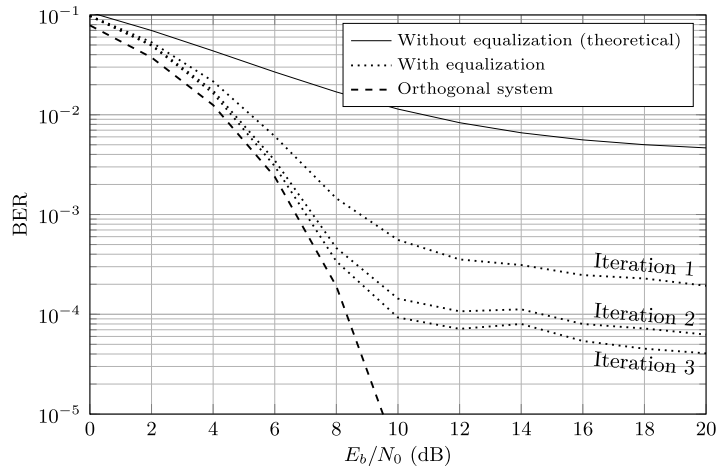


Fig. 10. BER as a function of E_b/N_0 for a multicarrier FTN system using a DFE, a density $\rho = 8/7$ and a TFL generator.

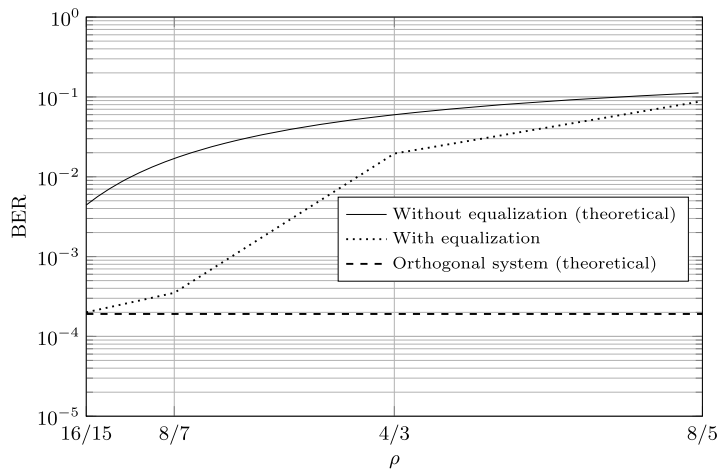


Fig. 11. BER as a function of ρ for a multicarrier FTN system using a DFE, $E_b/N_0 = 8$ dB and a TFL generator.

When used with a linear receiver and nothing else, Fig. 11 shows that this equalizer is not effective with high values of the density. However, it would be simple to get better performance by adding an error-correcting code, allowing for an improvement of the reliability of the estimated symbols. Another approach would consist in modifying this equalizer to let it work with soft inputs and produce soft outputs, as a way to integrate it in a turbo-equalization structure [10,8].

5. Conclusion

This article is based on the use of the optimal FTN linear multicarrier system derived in [4]. This system enables an increase in the signaling density in time and/or frequency. Consequently, spectral efficiency is improved as well, but this comes at the expense of unavoidable inter-pulse interference.

We show that a Gaussian approximation of the interference is accurate for the sake of a bit-error probability estimation, for which we give a closed-form expression. Two interference mitigation techniques are also presented, the first one involves an error-correction code with iterative decoding (LDPC code), while the second one is based on a per-block iterative decision feedback equalizer. The latter is shown to be very effective for low values of the density ($\rho \leq 8/7$), but suffers from the error propagation phenomenon for high values of the signal-to-noise ratio. It is shown through simulations that the Gaussian approximation of the interference term is also accurate for the sake of log-likelihood ratios computation, needed for example by LDPC codes and turbo-codes decoders, ensuring that $\rho \leq 8/5$. In this context, we introduce a method allowing for the prediction of the performance of this optimal linear system when associated with an error-correction code using iterative decoding, without requiring simulations, thus facilitating system design.

Future work may include interference mitigation by means of turbo-equalization [10], a more in-depth study of the statistical properties of the interference term, or an evaluation of this optimal linear system over time and/or frequency-selective channels.

References

- [1] H. Nyquist, Certain topics in telegraph transmission theory, *Trans. Amer. Inst. Electr. Eng.* 47 (2) (1928) 617.
- [2] W. Kozek, A.F. Molish, Nonorthogonal pulse shapes for multicarrier communications in doubly dispersive channels, *IEEE J. Sel. Areas Commun.* 16 (8) (1998) 1579.
- [3] F. Rusek, J.B. Anderson, The two dimensional MIMO limit, in: *International Symposium on Information Theory Proceedings*, 2005, p. 970.
- [4] C. Siclet, et al., On the study of faster-than-Nyquist multicarrier signaling based on frame theory, in: *Proc. International Symposium on Wireless Communications Systems, ISWCS*, 2014, p. 251.
- [5] J.G. Proakis, M. Salehi, *Digital Communications*, McGraw-Hill, 2008.
- [6] O. Christensen, *Frames and Bases: An Introductory Course*, Birkhäuser, 2008.
- [7] D. Pinchon, P. Siohan, Closed-form expressions of optimal short PR FMT prototype filters, in: *IEEE Global Telecommunications Conference (GLOBECOM'11) Proceedings*, 2011.
- [8] C. Berrou, et al., *Codes and Turbocodes*, IRIS, Springer-Verlag, Paris, 2010.
- [9] ETSI, EN 302 307 Digital Video Broadcasting (DVB); Second generation framing structure, channel coding and modulation systems for Broadcasting, Interactive services, News Gathering and other broadband satellite applications (DVB-S2), 2009.
- [10] C. Douillard, et al., Iterative correction of intersymbol interference: turbo-equalization, *Eur. Trans. Telecommun.* 6 (5) (1995) 507.